FABRICATION AND PREVASCULARIZATION OF EXTRACELLULAR MATRIX DERIVED SCAFFOLD FOR CARDIAC HEALING

An Undergraduate Research Scholars Thesis

by

SAMEEKSHA SHARMA

Submitted to the LAUNCH: Undergraduate Research office at
Texas A&M University
in partial fulfillment of requirements for the designation as an

UNDERGRADUATE RESEARCH SCHOLAR

Approved by
Faculty Research Advisor: Dr. Feng Zhao

May 2022

Major: Biomedical Engineering

RESEARCH COMPLIANCE CERTIFICATION

Research activities involving the use of human subjects, vertebrate animals, and/or biohazards must be reviewed and approved by the appropriate Texas A&M University regulatory research committee (i.e., IRB, IACUC, IBC) before the activity can commence. This requirement applies to activities conducted at Texas A&M and to activities conducted at non-Texas A&M facilities or institutions. In both cases, students are responsible for working with the relevant Texas A&M research compliance program to ensure and document that all Texas A&M compliance obligations are met before the study begins.

I, Sameeksha Sharma, certify that all research compliance requirements related to this Undergraduate Research Scholars thesis have been addressed with my Research Faculty Advisor prior to the collection of any data used in this final thesis submission.

This project did not require approval from the Texas A&M University Research Compliance & Biosafety office.

TABLE OF CONTENTS

ABSTRACT

Fabrication and Prevascularization of Extracellular Matrix Derived Scaffold for Cardiac Healing

Sameeksha Sharma
Department of Biomedical Engineering
Texas A&M University

Research Faculty Advisor: Dr. Feng Zhao
Department of Biomedical Engineering
Texas A&M University

Cardiovascular disease is a grievous and growing problem across the globe with limited therapeutic interventions available. This is due to the inability to replace fibrotic scar tissue which tends to accumulate and impair cardiac function. While stem cell-based regenerative therapies are promising, they are hindered by low survival and engraftment rates. These obstacles can be overcome by fabricating a complementary biomimetic scaffold that can support the development of an organized microvasculature and the growth of induced pluripotent stem cell derived cardiomyocytes (iPSC-CMs) to promote positive cardiac remodeling after myocardial infarction. The effectiveness of a cardiac scaffold relies on its ability to mimic the native myocardium by facilitating a multitude of cell-cell interactions and promoting the integration of implanted stem cells with the native myocardium. This has garnered attention on extracellular matrix cell sheets because they can form a completely biological, highly customizable, and tissue-specific scaffold. One of the cornerstones of designing a self-sustaining cardiac patch construct is supporting the development of a dense and highly organized microvasculature to meet the daily metabolic needs of implanted iPSC-CMs. The aim of this

project was to test the potential of iPSC-ECs to form such a robust and dense microvasculature on decellularized ECM cell sheets in comparison to the previously studied HUVECs. This was achieved by co-culturing bone marrow derived human mesenchymal stem cells (hMSCs) with iPSC-ECs or HUVECs on decellularized ECM cell sheets over ten days. The results of the ECM cell sheet fabrication demonstrated that human dermal fibroblasts (HDFs) can be used to produce a highly aligned ECM which retains its structural components after decellularization. Next, the prevascularization comparison between the hMSC/iPSC-EC and the hMSC/HUVEC revealed that iPSC-ECs could form a highly aligned microvasculature like the HUVECs. In fact, the average vessel length, diameter, and intercapillary distance in the hMSC/iPSC samples was more representative of the native myocardium than the hMSC/HUVEC control. Therefore, it can be concluded that co-culturing hMSCs and iPSC-ECs encompasses great promise for replicating the cardiac microvasculature and creating a perusable network of vessels that can support stem cell growth and maturation in cardiac patch constructs. This can propel regenerative medicine a step further by providing the biomimetic ECM scaffold the self-sustaining and robust microvasculature it needs to promote lasting cardiac repair healing for the growing number of patients in cardiovascular distress.

DEDICATION

I would like to dedicate this body of work to my parents, Atul Sharma and Rama Sharma. My dad once said that, if he could, he would want to go up with me to receive my award. Simply to share in the joy and the exhilaration of the moment. Until now that hasn't been possible. So, it's rather fitting to have him right here with me on my first publication. I'm eternally grateful to my mom for helping me become an articulate thinker and speaker by teaching me what it means to think deliberately and communicate effectively. Her advice and love will forever echo in my work.

ACKNOWLEDGEMENTS

Contributors

I would like to express my sincere gratitude to my mentor, Dr. Feng Zhao, for supporting this project. Despite being so occupied, she has always made time to provide practical guidance regarding research projects and new endeavors. Research is not always straightforward, but Dr. Zhao has a knack for honing into experimental details and learning from the result of each experiment. That is something I wish to learn from her, slowly but surely, as I navigate the arena of regenerative research. She continues to encourage me and work with me through my learning curves and I couldn't be more honored or grateful to be a member of her lab.

I also want to thank PhD students Te-An Chen and Dhavan Sharma. I thoroughly enjoy working with them every day because they never fail to be knowledgeable, reliable, and relatable. They have consistently been proactive about supporting my learning and made research an immensely meaningful experience for me beyond honing technical skills. It's when work stops feeling like work that you know you are part of a great team.

I would also like thank the Texas A&M Biomedical Engineering Department for challenging me with coursework and providing a plethora of diverse learning opportunities so I can emerge as a competent thinker and researcher.

All other work conducted for the thesis was completed by the student independently.

Funding Sources

This undergraduate research project was supported by Dr. Feng Zhao in the Texas A&M University Biomedical Engineering Department.

NOMENCLATURE

CMs	Cardiomyocytes
ECM	Extracellular Matrix
ESCs	Embryonic Stem Cells
HDFs	Human Dermal Fibroblasts
hMSCs	Human Mesenchymal Stem Cells
HUVECs	Human Umbilical Vein Endothelial Cells
iPSCs	Induced Pluripotent Stem Cells
iPSC-ECs	Induced Pluripotent Stem Cell Derived Endothelial Cells
MI	Myocardial Infarction

1. INTRODUCTION AND LITERATURE REVIEW

1.1 Extracellular Matrix Scaffold in Tissue Engineering

Tissue engineering solutions require a robust and biocompatible scaffold to effectively deliver regenerative therapeutics and induce lasting healing [1]. Regenerative therapies harness the infinite proliferative potential and selective differentiating ability of stem cells to repair injured tissue [2]. Wherein, scaffolds are constructs that support implanted stem cell survival, growth, maturation, and integration by serving as the delivery vehicles for regenerative therapeutics. Scaffolds provide a 3D mesh-like network that act as templates for tissue regeneration by closely emulating tissue microenvironments and facilitating cellular interactions [3]. This makes choosing a suitable scaffold a multifactorial decision. Properties, such as biocompatibility, porosity, topography among other physical and chemical properties must be taken into careful consideration when selecting an appropriate scaffold. Due to the innate complexity of tissues, biological tissue scaffolds have an edge over their synthetic counterparts. Unfortunately, synthetic scaffolds are not able to produce intact cell-cell junctions which causes disruptions in cell communication and even aggregation of cells that reduces the effectiveness of the therapy [4]. On the other hand, naturally derived tissue scaffolds can be easily customized to mimic the tissue-specific microenvironment. This aids in the differentiation and organized growth of implanted stem cells which optimizes sustainable tissue healing [5]. Among the biological tissue engineering options, ECM-based scaffolds are becoming subjects of vast research because they are naturally derived scaffolds with customizable structure and complex biophysical properties. Moreover, they naturally contain various important regulatory biochemical cues that influence cell shape, survival, proliferation, migration, and differentiation

[6]. Control over these delicate factors can play a pivotal role in enhancing implanted cell viability and producing lasting tissue regeneration [7].

1.1.1 Extracellular Matrix Scaffolds

ECM is complex connective network composed of proteins, polysaccharides, and glucosamine glycans (GAGs) and other natural macromolecules secreted by the tissue resident cells [8]. ECM is a biomaterial designed by nature with 600 million years of material optimization which makes it a highly desirable scaffolding material for regenerative therapies [9]. It provides an organized template for growth in tissues because it plays an indispensable role in cell motility which is a requirement for tissue development [10]. It serves as a reservoir for various macromolecules, including polysaccharides, growth factors, cytokines, and proteins guiding cell structure and function until the patient's own ECM can replace the implanted structure [11]. This allows ECM-based scaffolds to mimic tissue specific microenvironments and support the sustainable growth, maturation, and integration of stem cells into native tissue [12]. While single component ECMs made of collagen, fibrin, and hyaluronic acid are being tested for bone and skin regeneration they have individual shortcomings that can be addressed by using versatile ECM-based scaffolds.

1.1.1.1 Components of ECM Scaffolds

Some of the major structural components of ECM include collagen, fibronectin, laminin, elastin, and other short peptide sequences. Collagen is the among the most abundant protein in ECM [13]. While collagen has diverse isoforms, they share a commonality. Each isoform can construct complex functional superstructures which offer tissue strength and homeostasis [14]. Whereas fibronectin and laminin are essential glycoproteins that improve cell adhesion and migration [15]. Moreover, elastin is responsible for the overall flexibility of the ECM and

regulates cell behavior [16]. While there are several more proteins present in ECM, overall, these components work in unison to produce a stable scaffold that can promote and direct cellular growth better than a single component or synthetic scaffold.

1.1.1.2 Tissue Derived ECM

Single component scaffolds lack the overall biological complexity of native tissue microenvironments even though they can be produced in a large scale [17]. Some researchers have tried to address this challenge by using harvested ECM from whole tissues. Since the harvested ECM is tissue specific, it has been shown to promote implanted stem cell growth and differentiation and maintenance of their phenotypic characteristics [18]. While this methodology has been beneficial in characterizing various ECM components and understanding their interactions, these tissues carry the risk of pathogen transfer and can't be standardized because they are influenced by individual health conditions, such as age and illnesses. Moreover, ECM scaffolds derived from native organs continually face a challenge of organ donor scarcity and large batch-to-batch variation [19-20].

1.1.1.3 Cell Derived ECM

On the other hand, cell sheet derived ECM is easily customizable to patient needs without complications of possible pathogen transfer [21-22]. This provides a 3D model for scaffolding and can be used to generate various tissue-specific ECM by varying compositional resident cells and regulating their interactions [23]. Cell-derived ECM can curb the risk of pathogen transfer because. Moreover, the alignment and overall spatial distribution of cell derived ECM can also be regulated by using customized patterned substrate [24]. Studies and therapies are also not bound to the thickness of a harvested tissue and can stack the ECM cell sheets to produce a regenerative patch of a customizable thickness [25]. These reasons elaborate which cell derived

ECM sheets are a highly versatile scaffolding material that can be used in clinical studies and applied in future therapeutics.

1.2 Cardiac Tissue Engineering

1.2.1 Clinical Need: Myocardial Infarction

Cardiovascular disease has consistently been one of the leading causes of death worldwide. Out of the total cardiovascular disease deaths, nearly 60% occur due to the accumulation of scar tissue are caused by myocardial infarction (MI). According to the data published by the American Heart Association in 2021, an American adult dies of cardiovascular disease every 36 seconds [26]. MI is caused by a blockage in the coronary artery, which can lead to a reduction in the blood supply to the surrounding myocardium. This can severely impair cardiac function and precipitate the loss of highly specialized cardiomyocytes (CMs) [27]. The loss of the CMs is critically dangerous since they are cardiac muscle cells responsible for the heart's contractile forces and electrical signaling [28]. However, the adult body can hardly recover from ischemic injuries, like MI, because the body is unable to endogenously regenerate terminally differentiated CMs. Consequently, ischemia-induced loss of CMs leads to the accumulation of fibrotic scar tissue that can negatively remodel the heart and severely comprise its function [29]. In fact, MI can increase the chances of arrythmia and a more debilitating heart attack in the future, which is associated with less than a 50% chance of five-year survival [26].

1.2.2 Current Therapies

Currently the only therapeutic option for end-stage heart failure is heart transplantation [30]. This is an impractical solution for most patients due to the lack of healthy heart donors as well as chances of immune rejection and pathogen transfer [31]. Less acute heart failure is usually treated by prescribing blood thinners to prevent blood clots, inserting balloon stents to remove plaque formation, and bypass grafting. However, these methods serve to mitigate the

dangers of MI but are unable to restore healthy CMs in place of accumulated fibrotic scar tissue. This has produced a need for an external therapeutic that can stimulate and replenish injured cardiac tissue with healthy CMs post-cardiac distress. Researchers are currently striving to sustainably restore CMs using a regenerative cardiac patch construct that can stimulate controlled and lasting cardiac healing that meets clinical standards.

1.2.3 Prospective Stem Cell Therapies

1.2.3.1 Cell Injection Therapy

Since the adult human body can't endogenously regenerate CMs, each ischemic injury damages the cardiac tissue permanently and impairs its proper function. Researchers have been trying to use animal models to study the effects of injecting CMs on the site of cardiac injury to induce tissue repair and angiogenesis [32]. CMs for these therapies can be derived from various stem cell lineages, such as embryonic stem cells (ESCs), and from cardiac progenitor cells and injected onto the site of cardiac injury. It has been shown that an intramyocardial injection containing embryonic stem cells derived cardiomyocytes (ESC-CMs) improved cardiac function in mice with MI [32]. The injected ESC-CMs were able to integrate with the native CMs and form gap junctions for at least 12 weeks [33].

While intramyocardial injection therapies have led to improved cardiac function and a decrease in the negative remodeling of the heart in an animal model, intramyocardial injection has also been associated with a higher rate of arrhythmia [34]. This can be caused by insufficient structural integration of implanted stem cells or differences in electrical conduction velocities between implanted stem cells and the patient's native myocardium. Additionally, injecting stem cells makes it hard to control engraftment rate, cell orientation, and wave propagation, which are essential for regular cardiac function [35]. This makes injectable regenerative cardiac therapies unsustainable for clinical use which is why research is focused on fabricating a complementary

scaffold that can improve implanted stem cell survival, stimulate maturation, and avoid risk of arrhythmia.

1.2.3.2 Prevascularized ECM Cell Sheet Cardiac Patch

The need to produce a highly customizable and self-sustaining cardiac patch construct has sparked interest in ECM cell sheets. Using ECM cell sheet patches can make the cardiac patch construct more customizable because ECM can be generated in a highly aligned and tissue-specific manner using varied composition. Literature indicates that higher levels of fibronectin have been associated with increased cell proliferation and migration in cardiac tissue [36]. Fibronectin levels can be increased in the fabricated ECM by introducing resident cells that secrete more fibronectin. Similarly, increased presence of laminin too stimulates cardiac tissue regeneration [37]. This is because stem cell derived cardiomyocytes respond to spatial cues produced by laminin. CMs form elongated rod-shaped cells parallel to the lanes of laminin which can greatly improve the alignment of cells in the cardiac patch and enable them to generate more contractile force. The decellularized cell sheets can also be stacked to produce a cardiac patch of desired thickness. Work by other researchers has shown that cell sheet based cardiac patches can improve myocardial performance and impeded disease progression by discouraging the infarct from bulging [38]. Therefore, ECM cell sheets provide a more reliable way to improve stem cell survival, engraftment, and integration rate.

Additionally, ECM-based cell sheets are also capable of supporting a functional and perfusable vascular network which are making them increasingly clinically relevant. Since ECM cell sheets are natural and can be produced in a highly aligned manner, they provide endothelial cells (ECs) a conducive microenvironment for angiogenesis. Capillaries in native cardiac tissue have been observed to orient themselves in a uniaxial direction of myocardial fibers and wrap

around CMs [39]. ECM proteins allow ECs to form more focal adhesions, exhibit increased cell permeability, and form familiar cord like structures that emulate native vessels [40]. HUVECs have been shown to form dense and branched microvasculature on decellularized ECM cell sheets when co-cultured with hMSCs. The results of the study also described the formation of CD166 tracks which guided EC assembly and aligned microvessel formation [40]. However, prevacsularization of decellularized ECM hasn't been tested with hMSCs co-cultured with iPSC-ECs. This avenue is worth exploring because iPSCs are an ideal cell line for regenerative therapies given that they can be derived from patients, have an unlimited differentiating potential, and pose a minimal risk of immune rejection compared to HUVECs [41].

1.2.4 Future Perspective

Since all parts of the heart act as a single unit conducting significant contractile force and synchronized electrical signals, the implanted cardiac patch must meet these high mechanical and metabolic needs [42]. These conditions currently pose a challenge because there aren't standardized protocols on how to aid CM maturation and to enable patch integration with the systemic blood supply. Possible avenues to explore include understanding the mechanism of anastomosis, coculturing CMs with more tensile cell types, and mechanically stretching the cardiac patch to activate vessel branching. These are some prospective approaches that can be used to enhance CM maturation and integration to produce a self-sustaining cardiac patch [43].

1.3 Objective of Study

This thesis aimed to compare the potential of iPSC-ECs to form a comparable dense and organized microvascular network compared with previously tested HUVEsCs. This was accomplished by first creating a biomimetic and anisotropic ECM-based scaffold made from HDF cell sheets (Figure 1.1). The secreted ECM cell sheets were decellularized and

characterized using immunofluorescent staining to ensure that key structural features and components were retained after ECM decellularization. After characterization, the decellularized ECM samples were vascularized by seeding either hMSCs and iPSC-ECs or hMSCs and HUVECs to observe the differences in vessel development on day 3 and day 10 (Figure 1.1). This study is the first to explore the microvasculature produced by co-culturing hMSCs and iPSC-ECs. iPSCs were chosen for this study because they are a promising regenerative cell line that can be implanted into patients with minimal risk of immune rejection. Being able to cultivate a highly aligned and dense microvasculature on the decellularized ECM cell sheets with iPSC-ECs can bolster the compelling case for using ECM-based scaffolds for designing patient-specific self-sustaining cardiac patch.

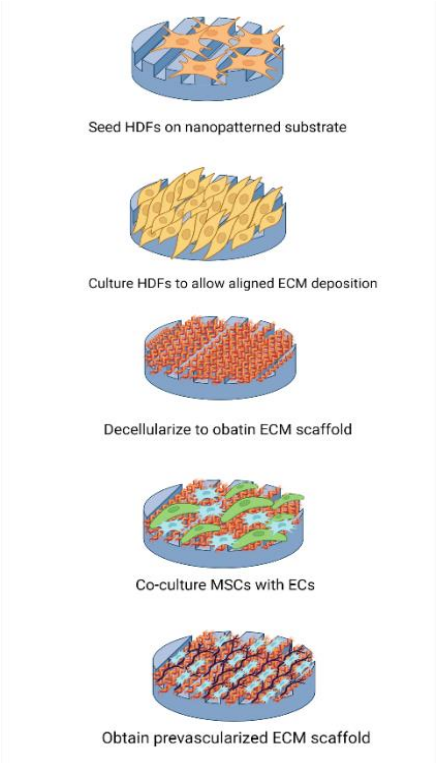

Figure 1.1: Objective of the study. Outlines two specific aims achieved in this study. The first aim is fabricating an ECM-based scaffold with anisotropic feature using HDFs. The second aim is investigating whether the HDF-derived ECM scaffolds can support the development of dense vasculature when coculturing hMSCs with iPSC-ECs as compared to the hMSCs and HUVEs control group. Created by Sameeksha Sharma on BioRender.com

2. METHODS AND MATERIALS

2.1 Fabrication of HDF Cell Sheets

Aligned polydimethylsiloxane (PDMS) substrates were created from nano-grated sheets of 450 nm width and 300 nm depth. The obtained PDMS was then coated with type I collagen (20 µg/mL) (Sigma-Aldrich, St Louis, MO) and dopamine-HCl (0.01% W/V). Passage 3 HDF(ATCC) at 10,000 cells/cm2 density were seeded onto the collagen and polydopamine coated PDMS and cultured for five weeks. The HDF were cultured with Dulbecco's modified eagle medium (DMEM) with 20% fetal bovine serum (FBS) and 1% penicillin-streptomycin (Penn-strep). Media was changed every 48 hours (h) for 5 weeks in the 24-well plate.

2.2 Decellularization of HDF Cell Sheets

The cultured cell sheets were then put into a decellularization solution composed of 1 M NaCl, 10 mM Tris (Bio-rad, Hercules, CA), and 5 mM Ethylenediaminetetraacetic acid (EDTA, Sigma, St Louis, MO). After which the 24-well plate was put on a shaker for 1 h at room temperature and rinsed thrice with phosphate buffered saline (PBS). The cell sheets were then put into a second decellularization solution containing 0.5% sodium dodecyl sulfate (SDS, Sigma), 10 mM Tris, and 5 mM EDTA and shaken for 30 minutes at room temperature. After which the cell sheets were washed thrice with PBS. Then submerged into FBS-containing medium for 48 h before being rinsed thrice with PBS.

2.3 Freezing and Storage of ECM

All liquid was first drained from the 24 well plate before being at -80 deg C in the liquid nitrogen tank.

2.4 ECM Characterization

The ECM derived from the HDF culture was first allowed to thaw at room temperature before immunofluorescence staining. Then the cell sheets were fixed and blocked with 1% bovine serum albumin (BSA, Sigma-Aldrich) in a 0.2% Triton X-100 (Sigma-Aldrich) solution. The samples were then incubated with collagen I, fibronectin, and laminin primary antibodies (Abcam, Cambridge, MA) for 1 hour followed secondary antibody staining for1 hour at room temperature. There were two identical samples for each type of staining. Representation images of the staining were then taken using the fluorescent microscope.

2.5 ECM Prevascualrization

Decellularized ECM samples were seeded with passage 3 hMSCs obtained from the Texas A&M University Health Sciences Center. The hMSCs were seeded at a 10,000 cells/cm^2 density and were cultured in α-minimum essential medium (α-MEM) with 20% FBS, 1% Penn-strep, and 1% L-glutamine (Thermo Fisher Scientific, Waltham, MA). The seeded hMSCs were subjected to hypoxia (5% O_2) condition for 7 days. After 7 days, the remaining samples were divided into two groups. Four wells were seeded with passage 3 human umbilical vein endothelial cells (HUVECs) (Lonza, Walkersville, MD). The HUVEC were seeded at 20,000 cells/cm^2 density on top of the hMSCs/ECM combination and would serve as the experimental control. The other four samples were seeded with passage 3 induced pluripotent stem cell derived endothelial cells (iPSC-ECs, P3) (Fujifilm, College Station, TX) at 20,000 cells/cm^2 density on top of the hMSCs/ECM combination. These co-cultures were maintained in normoxia (20% O_2) for 10 days and the endothelial cell growth media (EGM-2, Lonza) was changed every 48 h (Table 2.1).

Table 2.1: Well-plate layout for prevascularizing decellularized ECM samples.

Day 3	Day 10	Day 3	Day 10
MSC/iPSC-EC	MSC/iPSC-EC -EC	MSC/HUVEC	MSC/HUVEC
MSC/iPSC-EC	iP MSC/iPSC-EC SC-EC	MSC/HUVEC	MSC/HUVEC

2.6 Immunofluorescent Staining

The co-cultured prevascularized constructs were washed with PBS, fixed and co-stained with mouse polyclonal antibody against human CD31 (Abcam, Cambridge, MA) and rabbit polyclonal antibody against human CD 166 (Abcam, Cambridge, MA) for 1 h at room temperature. After carefully washing primary antibodies, samples were incubated with Alexa-flour 488 goat anti-mouse secondary antibody (Thermo Fisher), Alexa-Flour 555 goat anti-rabbit secondary antibody (Thermo Fischer), and Phallodin-Alexa flour 647 conjugated antibody (Thermo Fischer) for 1 h at room temperature in the dark. The samples were then incubated in 4′, 6-diamidino-2-phenylindole (DAPI, Sigma-Aldrich) solution for 5 minutes to stain cell nuclei. The samples were then mounted on cover glass using antifade mounting media and images were captured under the inverted fluorescent microscope (Zeiss Axio Observer) and the confocal microscope (Olympus FV1000). The images were processed with Image J software.

2.7 Microvasculature Analysis

The samples stained with CD31 revealed the growth of new vessels. This growth was quantified by comparing three key features across the two groups and the two time points. Image J was used to measure the length, dimeter, and the interpapillary distance in each sample. For each representative sample and feature, ten values were taken across a board spectrum of values

to encompass the diversity of data. The recorded data was assembled in Excel and then transferred into Spectrum data analysis software to create bar graphs. The graphs were formatted to analyze the standard deviation of the values to see whether there was a significantly significant difference in the length, diameter, and interpapillary distance of the samples.

2.8 Statistical Analysis

All statistical results were obtained from triplicated experiments. In software-based image analysis, five non-overlapping panels were randomly selected and analyzed from each sample to perform unbiased statistical analysis. The results were reported as mean ± standard deviation. Statistical comparisons between experimental groups were performed by one-way ANOVA and Tukey's post hoc test using GraphPad Prism software. Results were considered statistically significant for * $p < 0.05$, ** $p < 0.01$, *** $p < 0.001$, **** $p < 0.0001$.

3. RESULTS

To assess the results of the experiments, immunofluorescent staining was conducted. Each staining had two identical samples associated with it. The first set of staining characterized the major components of the decellularized ECM derived from the secretion of HDFs after five weeks of culturing. The second set of staining compared the development of vessels from Day 3 to Day 10 on the decellularized ECM with two experimental groups: (1) hMSC/iPSC-EC and (2) hMSC/HUVEC. Images were taken at 10x magnification to captsure a holistic representation of protein distribution and vessel development in the ECM.

3.1 ECM Characterization

Upon staining and characterization, the HDF-derived ECM demonstrated that it had been decellularized effectively without damaging the major structural components of the ECM. The anisotropic structure of collagen I, laminin, and fibronectin was verified using immunofluorescent staining after decellularization. The staining revealed that the collagen I, fibronectin, and laminin components were aligned with the underlying PDMS (Figure 3.1). This resulted in an overall well-aligned scaffold suitable for the subsequent seeding of cells for prevascularization comparison between hMSCs/HUVECs and hMSCs/iPSC-ECs sample groups. The images captured that collagen I and fibronectin created a highly aligned and elongated network on ECM (Figure 3.1, A and B). Laminin, however, was more localized within the samples (Figure 3.1, C). Finally, the DAPI staining data revealed that there were no cell nuclei present in the decellularized ECM which indicated that the samples were ready for the second objective of the study, prevascularization comparison.

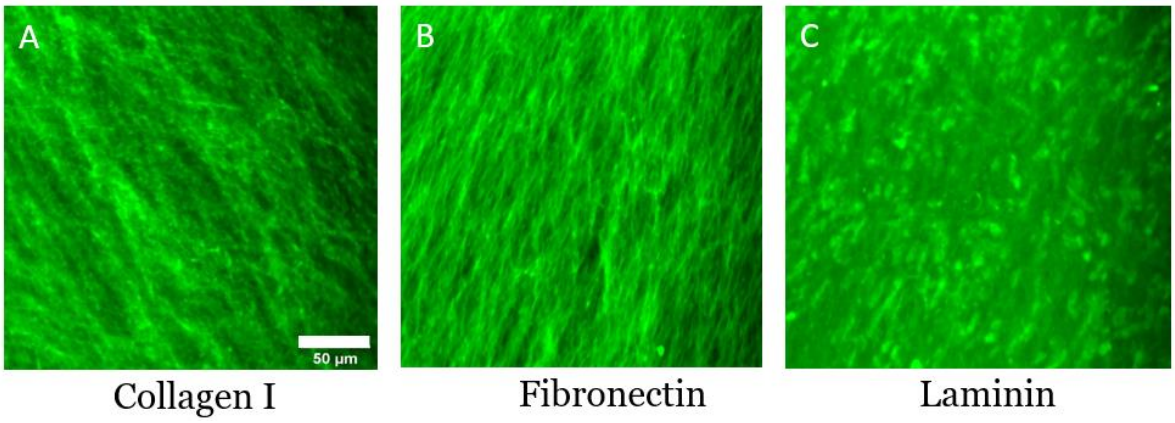

*Figure 3.1: Fluorescence microscopy of 3D HDF decellularized cell sheets. The HDFs were culture for 5 weeks at 20% oxygen. After five weeks, the cultures were fixed and stained to view major structural and regulatory components of the ECM. The above stains represent (**A**) Collagen I, (**B**) Fibronectin, and (**C**) Laminin at 10x magnification.*

3.2 Prevascularization of ECM

After decellularization, to conduct a prevascaulrization comparison, two identical samples from the hMSC/HUVEC and hMSC/iPSC-EC groups was conducted. The prevascularized samples were compared at day 3 and day 10. The samples were stained using CD 31, CD 166, F-actin, and DAPI to compare vessel development. Vessels were characterized by analyzing the length, diameter, and interpapillary distance of vessels in each sample. Images of the vessels was taken at 10x magnification with the confocal microscope (Olympus FV1000). While the images for CD166, F-actin, and DAPI were captured through the immunofluorescent microscope (Zeiss Axio Observer).

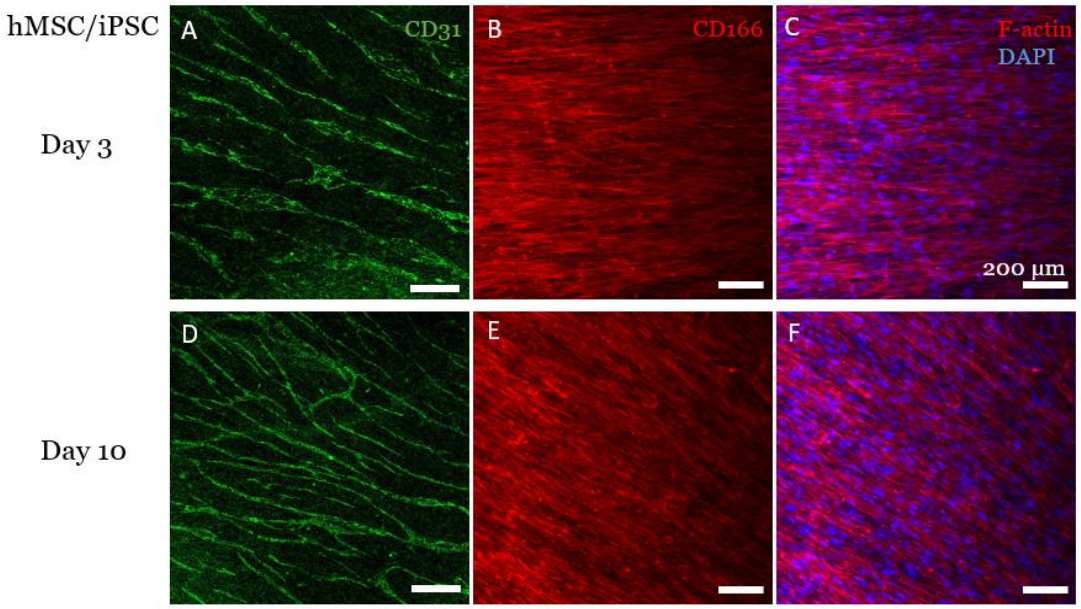

*Figure 3.2: The immunofluorescent staining of hMSC/iPSC-EC experimental group. The first panel of staining representation (**A**) CD31, (**B**) CD166, and (**C**) F-actin and DAPI on day 3. The following set of staining reveals (**D**) CD31, (**E**) CD166, and (**F**) F-actin and DAPI on day 10. The figure overarchingly depicts that samples have a denser and more branched vessel structure on day 10.*

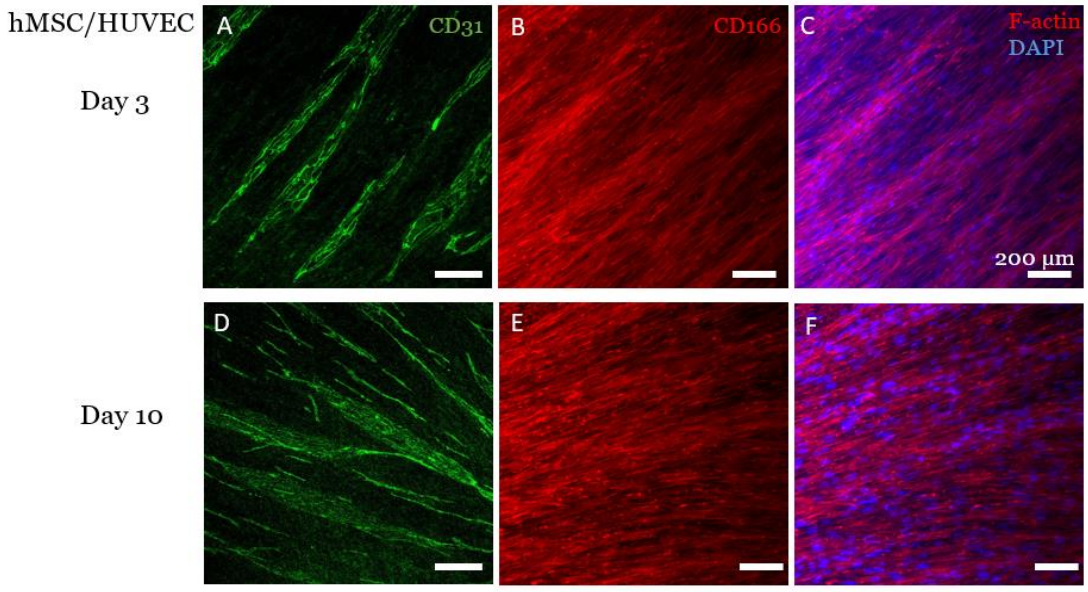

*Figure 3.3: The immunoflruorecnt staining of hMSC/HUVEC control group. The first panel of staining representation (**A**) CD31, (**B**) CD166, and (**C**) F-actin and DAPI on day 3. The following set of staining reveals (**D**) CD31, (**E**) CD166, and (**F**) F-actin and DAPI on day 10. This figure allows for the comparison in vessel development and morphology across experimental groups.*

Specific proteins were chosen to be stained because of their direct relevance in cell migration and vessel development which is further elaborated in the discussion section. The statistical analysis of the samples is based on CD31 staining which stained the endothelial cells, HUVEC or iPSC-EC, thus marking the development of tissues. There was on overall increase in vessel length, decrease in diameter and intercapillary distance noted across the day 3 and day 10 in the hMSC/iPSC-EC experimental group. The data for iPSC-EC samples revealed an increase from an average length of 708.28 μm on day 3 to 961.27 μm on day 10 (Figure 3.2 and 3.3, A, D). The average vessel diameter in the hMSC/iPSC-EC group on day 10 was 18.42 μm as compared to the 38.77 μm average diameter on day 10. Finally, a similar decrease in intercapillary distance was noted in the hMSC/iPSC-EC group from 63.71 μm on day 3 to 31.42 μm on day 10. While data was found to not be statistically significant because a wide range of values were used in the statistical analysis to get a holistic overview of the angiogenesis across all regions of the sample (Figure 3.4, A, B, C). This is attributed to the fact that not all regions in the samples had homogenous vessel development. Therefore, it is important to focus on the average values of length, diameter, and intercapillary distance to understand the holistic trend between the groups and time points. The range of values remain are insightful for optimizing future protocol to make more a homogenous prevascularized sample.

Quantifying the vessel development in the hMSC/HUVEC control group revealed a similar trend in the increase in average vessel length accompanied by a decrease in vessel diameter and intercapillary distance (Figure 3.2 and 3.3, A, D). Across the day 3 and day 10, the length of the vessels increased from an average of 558.58 μm on day 3 to 562.29 μm on day 10 in HUVEC. The decrease in diameter was more prominent across the two timepoints as the

average decreased from 52.09 µm on day 3 to 41.33 µm on day 10. Moreover, the average value of intercapillary distance for hMSC/HUVEC group on day 3 was 125.84 µm and it dropped to 67.66 µm, nearly half, by day 10.

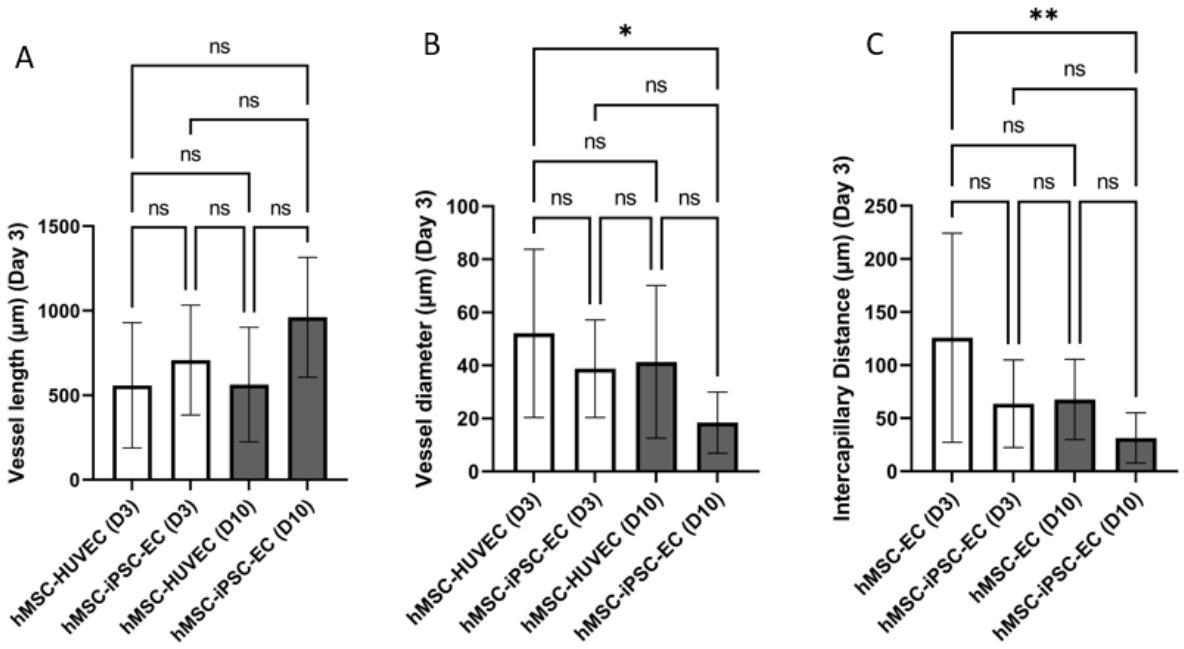

*Figure 3.4: This is a statistical comparison of the values in length, diameter, and intercapillary distance between the hMSC/iPSC-EC and the hMSC/HUVEC groups and across the two time points on day 3 and day 10 along with its statistical significance. (**A**) The average length of the vessels in each group. The MSC/iPSC-EC group had the longest vessels in comparison to the other groups. (**B**) The average diameter of the vessels in MSC/iPSC-EC in each group. (**C**) The intercapillary distance in each sample group. The average data trend revealed an increase in average vessel length, decrease in average vessel diameter and intercapillary distance from day 3 to day 10.*

These wide range of values were also observed across all samples and both timepoints since there wasn't homogenous development of vessels in all regions of the samples which caused variability in measurement. There are several parameters can be optimized, including cell density and incubator settings, which could have affected the homogeneity of vessel development. Despite there being no statistically significant significance in the comparisons between hMSC/iPSC-EC and hMSC/HUVEC group due to high variability, it is important to notice the overall trends of length, diameter, and intercapillary distance are indicated by the average data values (Figure 3.4,

A, B, C). The comparison between the hMSC/iPSC-EC and hMSC/HUVEC group on day 3 reveals that that the iPSC group had longer average vessel length, small diameter, and less intercapillary distance than the HUVEC control group. This trend was also present in the day 10 samples revealing that the hMSC/iPSC-EC experimental group was more representative of native myocardial features that than the control HUVEC samples. This can also be visually corroborated when looking at the staining data.

The other staining results were analyzed qualitatively to aid in the interpretation of the statistics derived from CD31 staining and overall vessel development data. The staining of CD166 revealed a homogenous network with organized alignment in the same direction as the ECM (Figure 3.2 and 3.3, B, E). Moreover, a dense and aligned network of F-actin was also observed since it an integral feature of the ECM upon which the hMSCs and two different types of ECs were scaffolded. Finally, cell nuclei were stained using DAPI which showed that there was a dense and healthy presence of hMSC and endothelial cells in both groups (Figure 3.2 and 3.3, C, F).

4. DISCUSSION

4.1 Interpreting Results

The eventual application of self-sustaining regenerative cardiac patches is highly dependent on being able to replicate the dense microvasculature present in the myocardium. Research has shown that vascular development and density is influenced by the scaffolding material which is why this study focused on fabricating naturally derived ECM and conduct a prevascularization study to better understand the stages of angiogenesis on ECM scaffolds over 10 days [44]. This was achieved by producing a highly aligned ECM generated from HDFs to observe ECM composition post-decellularization to ensure that the integrity of the ECM scaffold was maintained before conducting a prevascularization comparison. For the second aim, the prevascularization comparison was conducted between two sample groups consisting of hMSC/iPSC-EC and hMSC/HUVEC seeded on the decellularized ECM. The test aimed to compare the status of angiogenesis between the two sample groups at two timepoints on day 3 and day 10. The immunofluorescent spectroscopy revealed that there was an increase in vessel formation and a distinct change in their morphology which is more consistent with native cardiac vessels.

4.1.1 ECM Characterization

The characterization of the derived ECM demonstrated that the seeded HDF cells could sense of the topography of a patterned PDMS substrate which encourages to grow in an aligned manner along the nano grated patterns. Being able to replicate such high levels of structural alignment in fabricated ECM is promising because this indicates that the ECM can mimic tissue-specific spatial micromovements that can enhance stem cell growth, survival, and integration

into the native tissue. The characterization also revealed that the ECM can retain its composition and has the major structural components after being completely decellularized. Since collagen I, fibronectin, and laminin are structurally integral to cell organization and migration, these proteins were stained using antibody staining. The samples revealed a thick and aligned network of collagen and fibronectin as has been observed in previous studies [45]. This is expected since collagen I is the most abundant protein in ECM and fibroblasts are considered a major collagen I source which is why they were selected for ECM deposition [46]. Observing highly aligned collagen I network enhances the possibility the ECM is a scaffold that can enhance 3D cell attachment and implanted stem cell growth. Similarly, a dense fibronectin network also indicates various cellular activities vital for normal tissue function such as cell adhesion and migration which are crucial to the subsequent prevascularization comparison [47]. Whereas laminin comes from a family of glycoproteins located in the basal lamina of cells to regulate communication between cells and cell surface receptors as well as other ECM components. It has been shown to self-assemble into localized aggregates which serve to communication bridges between molecules [48]. Overall, the characterization of the decellularized HDF cell sheet derived ECM demonstrates that ECM is highly versatile and aligned scaffold made from a composite of glycoproteins that can support cell structure as well as provide higher levels of organization for angiogenesis.

4.1.2 ECM Prevascularization Comparison

The prevascularization test was conducted on hMSC/iPSC-EC with hMSC/HUVEC serving as the experimental control. These cells were co-cultured on the decellularized ECM for ten days and the vessels of two identical samples from each group were stained on day 3 and ay 10. The time points were chosen based on previous literature to make an analogous comparison

between the group of interest consisting of hMSC/iPSC-EC and the hMSC/HUVEC control group.

Overall, four proteins were stained to observe new vascular growth and get an insight into the mechanism of its development. Prevascularization samples were stained with CD31, CD166, F-actin, and DAPI to compare results with previous work and deem whether the observations were consistent. CD31 tracks endothelial cells so it was chosen to record the development of new vessels in the prevascularization samples from both the hMSC/iPSC-EC and hMSC/HUVEC groups. Previous research has shown that in HUVEC matrix proteolytic activity can influence EC migration and angiogenesis [49]. This has made CD 166 a protein of interest because it is known to activate and regulate MMP-2 which becomes significantly activated in aligned ECM samples during the initial stages of angiogenesis. It was expected that the MSC/HUVEC samples would reveal track marks made by CD166 along the highly aligned ECM which would then be followed by endothelial cells during vessel development [50], However, the staining of CD166 didn't reveal any visually distinct track marks made by CD166 along the ECM that were also stained with CD31 showing endothelial cell migration along the tracks. Despite that, the resulting vessels were highly aligned like the underlying ECM. On the other hand, F-actin and cell nuclei were also stained to gain a better understanding of the ECM structure and the overall density of cells in each sample. The staining demonstrated that the structure of the ECM was not compromised and still had a high degree of organization and alignment to guide vessel growth.

The endothelial cells (HUVECs and iPSC-ECs) were co-cultured with hMSCs because previous work has shown that hMSCs co-cultured with HUVEC yields a highly organized and dense microvasculature with both endothelial and perivascular phenotypes being expressed [50].

This was consistent with the findings of this study. Although the differences in length, vessel diameter, and intercapillary distance were not found to be statistically significant, given the broad range of values, it is important to highlight that the iPSC-EC experimental group yielded longer, thinner, and denser vessels the HUVEC control group. In fact, the average intercapillary distance in the MSC/iPSC-EC group, 31.40 µm, resembles the intercapillary distance of the native myocardium, typically 20 µm. The statistical significance of the measured features can be proven in a future study my optimizing protocol to ensures a denser and more homogenous patch to make a starker comparison between the MSC/iPSC-EC group and the MSC/HUVEC control group.

Overarchingly, this study demonstrated that the hMSC/iSPC-EC group created a more suitable microvasculature than the hMSC/HUVEC control group. These results are promising for the eventual clinical application of cardiac patches because regenerative medicine requires biomimetic scaffolds that can support the growth and integration of suitable stem cell lines with minimal risk of immune rejection in host tissue. As discussed earlier, iPSCs are an ideal candidate for patient-specific regenerative therapies because of their high proliferative potential and ability to differentiate into numerous cell types. Therefore, iPSCs are the key to designing highly individualized cardiac patch constructs with aligned microvascular features [51]. Moreover, the versatility of ECM along with other optimizations in technique can help researchers obtain a self-sustaining patient-specific cardiac patch that can connect with the systemic blood supply and significantly improve cardiac regenerative outcomes.

5. CONCLUSION

Overall, the results demonstrated that a highly aligned and compositionally versatile ECM can be naturally derived from HDFs, which can mimic tissue-specific microenvironment to promote angiogenesis. This was tested by revascularizing decellularized ECM cell sheets and co-culturing it with MSCs and two different types of ECs which yielded a dense microvasculature. It is important to highlight that the experimental group containing MSCs and iPSC-ECs yielded a longer, thinner, and denser vasculature as compared to the MSCs with HUVECs control group on both day 3 and day 10. The vessels produced from iPSC-ECs presented an aligned and narrow morphology demonstrating its capacity to form organized vessels and meet the daily metabolic needs of implanted stem cells in a cardiac patch construct.

5.1 Short-term Focus

While the results of the ECM characterization and the prevascularization study were promising there is a urgent need to expand the understanding of other microvasculature features, such as degradation and cytokine expression. Although the results of this study did not confirm that CD166 creates tracks in the ECM for endothelial cells to follow during angiogenesis, there are serval parameters that can be optimized to reassess results more carefully. Conditions such ECM freezing, incubator settings, staining conditions, and cell seeding density can be altered to improve vascular development to produce a denser microvasculature. Being able to conduct more experiments will better elucidate the mechanism underlying angiogenesis and how other ECM components interact and influence vessel formation. Having an insight into this will help standardize protocols to produce more angiogenesis microenvironments because a robust vasculature is an integral part of self-sustaining regenerative construct. The mechanism of

angiogenesis and morphology of new vessels can also be compared across multiple cell lines to see which option or combination yields the most robust and dense microvasculature for creating an individualized ECM-based cardiac patch to promote endogenous cardiac healing.

5.2 Long-term Possibilities

While developing a microvasculature is critical, there are more avenues of study that need to be ins and elucidated to make regenerative cardiac patches a clinical reality. This includes investigating the survival and interactions of iPSC-CMs on prevascularized ECM scaffolds [52]. When designing these studies, it will be important to take factors, such as iPSC-CM alignment, density, and maturation into close consideration to ensure low risk of mechanical failure and arrythmias [53]. Moreover, there must remain an emphasis on optimizing methodology to improve cell-engraftment and maturation because those are indispensable conditions that must be demonstrated before clinical application.

Researchers also need to find way of storing ECM for long periods of time without compromising its structural integrity while preserving its endogenous biochemical cues. Looking further into the future, researchers must reach consensus on an optimized and standardized approach for creating clinically relevant cardiac patches [54]. This can be made possible by further studying ECM-based scaffolds given its highly aligned structure and ability to closely replicate the native tissue microenvironment. Additionally, this study demonstrated that ECM-based scaffolds are also capable of supporting a dense microvasculature which can be optimized to resemble the native myocardium. Being able to devise a self-sustaining cardiac patch will overcome several challenges that plague regenerative medicine right now by minimizing the need for organ donors, making pathogen screening easier, and producing a patient-specific patch that stimulates cardiac healing.

REFERENCES

1. Hosseinkhani, M., et al., *Tissue engineering scaffolds in regenerative medicine*. World J Plastic Surg, 2014. **3**(1): p. 3-7.

2. Ghasemi-Mobarakeh, L., et al., *Structural properties of scaffolds: Crucial parameters towards stem cells differentiation*. World J Stem Cells, 2015. **7**(4): p. 728-44.

3. Anderson, JM., et al., *Foreign body reaction to biomaterials*. Semin Immunol, 2008. *2*0: p. 86–100

4. Chan BP, Leong KW. *Scaffolding in tissue engineering: general approaches and tissue-specific considerations*, 2008. **4**(4): p. 467-79.

5. Yi, S., et al., *Extracellular matrix scaffolds for tissue engineering and regenerative medicine*. Curr Stem Cell Res Ther, 2017. **12**(3): p. 233-246.

6. Agmon G, et al., *Controlling stem cell behavior with decellularized extracellular matrix scaffolds*. Curr Opin Solid State Mater Sci, 2016. **20**(4):193-201.

7. Daley, WP., *Extracellular matrix dynamics in development and regenerative medicine*. J Cell Sci, 2008. **121**(3): p. 255-64

8. Yue, B., *Biology of the Extracellular Matrix: An Overview*. J Glaucoma, 2015. **23**(8): p. 20-23.

9. Assuncao, M., et al., *Cell-derived extracellular matrix for tissue engineering and regenerative medicine*. Front Bioeng Biotechnol, 2020. **8**: p. 602009.

10. Kim Y, et al., *Extracellular matrix revisited: roles in tissue engineering*. Int Neurourol J, 2016. **20**(1): p. 23-29.

11. Tallawi M, et al., Strategies for the chemical and biological functionalization of scaffolds for cardiac tissue engineering: a review. J R Soc Interface, 2015. **12**(108): p. 20150254.

12. Yi H, et al., Tissue-specific extracellular matrix promotes myogenic differentiation of human muscle progenitor cells on gelatin and heparin conjugated alginate hydrogels. *Acta Biomater*, 2017. **62**: p. 222-233.

13. Glowacki J, et al., *Collagen scaffolds for tissue engineering*. Biopolymers, 2008. **89**(5): p. 338-44.

14. Frantz, C., et al., *The extracellular matrix at a glance.* Journal of cell science, 2010. **123**(24): p. 4195-4200.

15. Stoffels JM, et al., *Fibronectin in tissue regeneration: timely disassembly of the scaffold is necessary to complete the build*. Cell Mol Life Sci, 2013. 70(22): p. 4243-53.

16. Miner, JH., *Laminin Function in Tissue Morphogenesis*. Annu Rev Cell Dev Biol, 2004. **20**: p. 255-84.

17. Sell, S.A., et al., *The use of natural polymers in tissue engineering: a focus on electrospun extracellular matrix analogues.* Polymers, 2010. **2**(4): p. 522-553.

18. Hellewell, A., et al., *A rapid scalable method for the isolation, functional study, and analysis of cell-derived extracellular matrix*. J Vis Exp, 2017. (119): p. 55051.

19. Tzila, D., et al., *Extracellular matrix hydrogels originated from different oragns mediate tissue-specific properties and function*. Int. J Mol. Sci., 2021. 22: p. 11624.

20. Krishtul, S., *Processed tissue-derived extracellular matrix: tailored platforms empowering diverse therapeutic applications*. Adv. Funct. Mater., 2019. 30, p. 1-26.

21. Bar, A., *Inducing Endogenous Cardiac Regeneration: Can Biomaterials Connect the Dots? Frontiers in Bioengineering and Biotechnology*, 2020. 8; p. 126.

22. Xing, Q., et al., *Decellularization of fibroblast cell sheets for natural extracellular matrix scaffold preparation*. Tissue Eng Part C Methods, 2015. **21**(1): p. 77-87.

23. Nelson, C.M. and M.J. Bissell, *Of extracellular matrix, scaffolds, and signaling: tissue architecture regulates development, homeostasis, and cancer*. Annu. Rev. Cell Dev. Biol., 2006. **22**: p. 287-309.

24. Grenier, G., et al., *Tissue reorganization in response to mechanical load increases functionality*. Tissue Eng., 2005. **11**(1-2): p. 90-100.

25. Haraguchi, Y., et al., *Electrical coupling of cardiomyocyte sheets occurs rapidly via functional gap junction formation*. Biomaterials, 2006. **27**(27): p. 4765-4774.

26. Sharma, D., et al., *Constructing biomimetic cardiac tissues: a review of scaffold materials for engineering cardiac patches*. Emergent materials, 2019. **2**(2): p.181-191.

27. Virani, S.S., et al., *Heart disease and stroke statistics—2021 update: a report from the American Heart Association.* Circulation, 2021. **143**(8): p. 254-743.

28. Walker, C., and Francis G. Spinale, *The structure and function of the cardiomyocyte: a review of fundamental concepts*. JTCVS, **118**(2): p. 375-382.

29. Yue, L., et al., *Molecular determinants of cardiac fibroblast electrical function and therapeutic implications of atrial fibrillation*. Cardiovasc. Res., 2011. **89**(4): p. 744-53.

30. Alraies, M., and Peter Eckman, *Adult heart transplant: indications and outcomes*. J Thorac Dis, 2014. **6**(8): p. 1120-1128.

31. Harris, C., et al., *Heart transplantation*. Ann Cardiothorac Surg, 2018. **7**(1): p. 172.

32. Tompkins, B.A., et al, What is the future of cell-based therapy for acute myocardial infarction. Circ Res., 2017. **120**(2): p. 252-255.

33. *van* Laake, L.W., et al., *Human embryonic stem cell-derived cardiomyocytes survive and mature in the mouse heart and transiently improve function after myocardial infarction.* Stem cell research, 2007. 1(1): p. 9-24.

34. Almeida, SO., Arrythmia in Stem Cell Transplantation. Cardiac Electrophysiology Clinics, 2015. 7(2): p 357-370.

35. Abate, A., et al., *Acute myocardial infarction and heart failure: role of apoptosis.* The international journal of biochemistry & cell biology, 2006. 38(11): p. 1834-1840.

36. *Esmaaeii, H., Engineering Extracellular Matrix Proteins to Enhance Cardiac Regeneration After Myocardial Infarction. Front Bioeng Biotechnol, 2021. 8: p. 611936.*

37. *Takkaki, S., Laminin-221 Enhances Therapeutic Effects of iPSC-Derived 3-D Engineering Cardiac Tissue Transplantation in a Rat Ischemic Cardiomyopathy Model. Journal of the American Heart Association, 2020. 9(16): p.e015841.*

38. Shimizu, T., et al., *Electrically communicating three-dimensional cardiac tissue mimic fabricated by layered cultured cardiomyocyte sheets.* Journal of biomedical materials research, 2002. 60(1): p. 110-117.

39. Kaneko, N., et al., *Three-dimensional reconstruction of the human capillary network and the intramyocardial micronecrosis*. Am J Physiol Heart Circ Physiol, 2011. 300: p. H754-H61.

40. Qian, Z., et al., *Engineering stem cell cardiac patch with microvascular features representative of native myocardium*. Thernostics, 2019. **9**(8): p. 2143-2157.

41. Wu, S. and Konrad Hochedlinger, *Harnessing the potential of induced pluripotent stem cells for regenerative medicine*. Nat Cell Biol., 2011. **13**(5): p. 497-505.

42. Zhang, J., *Can We Engineer a Human Cardiac Patch for Therapy?* Circulation Research, 2018. **123**: p. 244-265.

43. *Hisayuki, H., Therapeutic Approaches for Cardiac Regeneration and Repair. Nat Rev Cardiol, 2018. **15**(10); p. 585-600.*

44. Stratman, A.N., et al., *Pericyte recruitment during vasculogenic tube assembly stimulates endothelial basement membrane matrix formation*. Blood, 2009. **114**: p. 5091-101.

45. Novoseletskaya, E., et al., *Mesenchymal stromal cell-produced components of extracellular matrix potentiate multipotent stem cell response to differentiation stimuli*. Front Cell Dev Biol, 2020. **8**: p. 555378.

46. Kendall, R., and Carol Feghali-Botswick, *Fibroblasts in fibrosis: novel roles and mediators*. Front. Pharmacol., 2014. **5**: pg. 123.

47. Hsiao, C., *Fibronectin in cell adhesion and migration via N-glycosylation*. Oncotarget, 2017. **8**(41): p. 70653-70668.

48. Tsuruta, D., *Laminin-332-integrin: a target for cancer therapy?* Curr Med Chem, 2008. **15**(20): 1968-1975.

49. Du., P., *Vascular morphogenesis of human umbilical vein endothelial cells on cell-derived macromolecular matrix microenvironment*. Tissue Eng Part A, 2014. **20**(17-18): 2365-2377.

50. Sharma, D., et al., *Upgrading prevascularization in tissue engineering: A review of strategies for promoting highly organized microvascular network formation*. Acta biomaterialia, 2019. **95**, p. 112–130.

51. *Menasche, P., Towards a Clincal Use of Human Embryonic Stem Cell-Derived Progenitors: A Translational Experience. Eur Heart J, 2014. 36(12): p. 743-750.*

52. Zhang, J., *Engineering Tissue Patch for Cardiac Cell Therapy*. Curr Treat Options Cardiovasc Med, 2015. **17**(8): p. 399.

53. Herron, T., *Extracellular matrix mediated maturation of human pluripotent stem cell derived cardiac monolayer structure and electrophysiological function*. Circ Arrthyhm Electrophysiol, 2016. **9**(4): p. 3638.

54. Singh V.K., et al. *Induced pluripotent stem cells: applications in regenerative medicine, disease modeling, and drug discovery*. Front Cell Dev Biol., 2015. **3**(2): p. 2.